# Calorimetric study of the giant magnetocaloric effect in $(MnNiSi)_{0.56}(FeNiGe)_{0.44}$

E. Palacios,[1,*] R. Burriel,[1] and C. L. Zhang[2]
[1]*Department of Condensed Matter Physics and Instituto de Ciencia de Materiales de Aragón, CSIC–University of Zaragoza, Pedro Cerbuna 12, 50009 Zaragoza, Spain*
[2]*School of Science, Jiangnan University, WuXi 214122, China*

(Received 3 January 2021; accepted 18 February 2021; published 1 March 2021; corrected 26 March 2021)

$(MnNiSi)_{0.56}(FeNiGe)_{0.44}$ belongs to a new family of alloys, similar to MnAs, showing a magnetostructural first-order transition near room temperature with large latent heat and magnetocaloric effect (MCE). From isothermal magnetization, remarkable values of the entropy change have been reported, such as $|\Delta S_T| = 11.5$ J/kg K at 290 K for the small field change of 1 T, or $|\Delta S_T| = 70.1$ J/kg K for 5 T on a slightly different composition. Strangely, this last value almost doubles that obtained from the Clausius-Clapeyron equation. Therefore, a very detailed set of calorimetric determinations have been made including heat capacity by adiabatic and differential scanning calorimetry (DSC), and direct measurement of the heat absorbed on isothermal demagnetization for several magnetothermal histories of the sample. We found high values of $|\Delta S_T| = 45.7$ J/kg K at 289.4 K for a field change of 7 T, for a sample previously cooled to a low temperature and then heated under magnetic field to the target temperature. This value is high but very far from previously reported data, which happened to be nonphysical but obtained from a very frequently used, but incorrect, experimental protocol to determine $\Delta S_T$ from magnetization, via the Maxwell relation. The spurious contribution has been analyzed and computed, explaining the nonphysical reported values. The strong thermal and magnetic hysteresis of 8.4 K and 8.3 T, respectively, make this alloy useless for magnetic refrigeration, but the results encourage searching for other derivatives with lower hysteresis which could have even higher $|\Delta S_T|$.

DOI: 10.1103/PhysRevB.103.104402

## I. INTRODUCTION

Refrigeration by adiabatic demagnetization is a standard procedure, known since the 1930s [1], to reach temperatures below 1 K. The application to refrigeration near room temperature (RT) needs ferromagnetic substances containing high magnetic moment density, atoms with high angular momentum $J$ (which implies a large magnetic entropy reduction on an applied field), low anisotropy, and with Curie temperature near RT. All these conditions are fulfilled by gadolinium (Gd) metal, with $T_C = 293$ K, $J = 7/2$, $M = 7\mu_B$/f.u., and virtually no anisotropy, having a maximum isothermal entropy decrement $\Delta S_T = -10.5$ J/kg K and a maximum adiabatic temperature increment $\Delta T_{ad} = 12$ K at 295 K, for an external field variation from zero to $B = 5$ T [2]. The real possibility of improving these properties is with an alloy having a first-order magnetostructural transition at some temperature $T_t$. In this case, near $T_t$ a weak or moderate field can produce the full discontinuous entropy change. Moreover, this change involves magnetic and, especially, nonmagnetic (phononic or electronic) contributions to the entropy. Therefore, the entropy change is not limited to $k_B \ln J$ per magnetic atom, although this value is hardly reached in actual materials.

After the so-called "giant magnetocaloric effect" in $Gd_5Si_2Ge_2$ [3], some other families with first-order transition were studied in the 2000–2010 decade, such as $La(Fe,Si)_{13}$ [4], MnAs [5], MnFe(P,Si,Ge) [6], $Mn_3GaC$ [7,8], Heusler alloys Ni-Mn-$A$ ($A$ = Sn, In, Sb, Ga) [9], and others. Since 2010, many papers have been published about every family. Most works propose improvements in the known families by small changes in composition or by atomic substitution without substantial modifications of the crystal structures. An extensive monography about materials with high magnetocaloric effect (MCE) is in the book by Tishin and Spichkin [10]. A more recent review can be found in [11].

This work deals with the MCE of the family $(MnNiSi)_{1-x}(FeNiGe)_x$, especially the values of $\Delta S_T$ directly determined and also obtained from heat capacity. The results show that those deduced from isothermal magnetization, very frequently have no physical sense because of an incorrect application of the Maxwell relation. Section II deals with previous results in the family. Section III covers a discussion of the experimental calorimetric techniques. Section IV shows the MCE deduced from several methods. Sections V and VI are discussion and conclusions.

## II. THE FAMILY $(MnNiSi)_{1-x}(FeNiGe)_x$

Mn$T$Ge ($T$ = Co, Ni) undergoes a martensitic transition at high temperatures, in paramagnetic state, from an orthorhombic TiNiSi-type structure (space group *Pnma*) to a hexagonal $Ni_2In$-type structure ($P6_3/mmc$), with a large jump in volume. Replacing some Mn with Cr or interstitial B, Trung *et al.* obtained compounds with a magnetostructural transition from the ferromagnetic (FM) TiNiSi type to the paramagnetic

*elias@unizar.es

 

(PM) $Ni_2In$ type near RT [12,13]. MnNiSi has a very high transition temperature $T_t \simeq 1200$ K and FeNiGe is always hexagonal, but it has been shown that the chemical alloy of both intermetallic compounds with similar proportions, $(MnNiSi)_{1-x}(FeNiGe)_x$ with $0.36 \leqslant x \leqslant 0.52$, gives a phase with a magnetostructural transition near RT [14]. The transition can be induced by a magnetic field and a large isothermal entropy change has been reported, $|\Delta S_T| = 11.5$ J/kg K at 290 K, for a moderate field of 1 T, as deduced for the sample with $x = 0.44$ from magnetization measurements [14], via the well-known Maxwell relation

$$\left(\frac{\partial S}{\partial B}\right)_T = \left(\frac{\partial M}{\partial T}\right)_B \Rightarrow \Delta S_T = \int_0^B \left(\frac{\partial M}{\partial T}\right)_B dB. \quad (1)$$

On the other hand, the classical Clausius-Clapeyron (CC) equation, which relates the slope of the transition line in the $B/T$ diagram with the entropy and magnetization changes at the transition, $dB_t/dT_t = -\Delta S/\Delta M$, gives also a high $|\Delta S| \simeq 55$ J/kg K for the entropy jump at the transition, assuming $dB_t/dT_t \simeq 1$ T/K as deduced from [14]. All these preliminary results suggest that $(MnNiSi)_{1-x}(FeNiGe)_x$ is a new family of rare-earth free alloys with interest in magnetocaloric refrigeration. Dutta *et al.* [15] have recently reported a "colossal" MCE, with $-\Delta S_T = 70.1$ J/kg K for $\Delta B = 5$ T, in an alloy with $x = 0.47$. Also "giant magnetocaloric effect" has been found in the very closely related alloy $(MnNiSi)_{1-x}(Fe_2Ge)_x$ with peak values $-\Delta S_T \simeq 49.3$ J/kg K [16] and $-\Delta S_T \simeq 57$ J/kg K [17] for 5 T. Hanggai *et al.* [18] give a table of MCE parameters of isostructural alloys with different compositions, most of them obtained from magnetization data. Zhang *et al.* [14] already mentioned that the determination of $\Delta S_T$ from isothermal magnetization can overestimate its values, which puts in question this type of determinations.

Indeed, fundamental thermodynamic considerations show that the way in which the Maxwell relation is commonly applied to the standard isothermal $M_T(B)$ measurements in compounds with sharp hysteretic first-order transitions necessarily leads to a spurious spike which has nothing to do with the isothermal entropy increment, nor with the MCE, but with an incorrect experimental procedure [19]. In other compounds, such as Heusler alloys, the transition is not so sharp and the spurious contribution does not have the spike shape. This case was extensively discussed for $Ni_{50}CoMn_{36}Sn_{13}$ [20]. This alloy has inverse magnetocaloric effect in the temperature range of the martensitic transition, $\Delta S_T > 0$ for $\Delta B > 0$, since the high temperature phase (austenite) is ferromagnetic while the low temperature one (martensite) is paramagnetic. Therefore, the total entropy increment is positive, since the minimum free energy imposes a higher entropy to the high temperature phase, although the magnetic contribution decreases with the field. In this case, $\Delta S_T > 0$, but the magnetic contribution is negative, $\Delta S_M < 0$. They do not have any evident relation, since the phononic or electronic entropy change found in other nonmagnetic shape memory alloys is similar to that found in this case.

Likewise, the classical CC equation is not valid either when there is hysteresis. Instead, a modified version should be used [21],

$$\frac{dB_t}{dT_t} = -\frac{\Delta S}{\Delta M} + \frac{1}{\Delta M}\frac{dE_{\text{diss}}}{dT_t}, \quad (2)$$

where the dissipated energy, $E_{\text{diss}}$, is the area of a hypothetical isothermal hysteresis loop in which, on magnetization, the transition occurs at the actual transition field value $B_{tm}$ and, on demagnetization, occurs at the field of thermodynamic equilibrium between the PM and FM phases, that is, when the specific free energy is the same for both phases.

After these considerations, a study of the magnetostructural transition by calorimetric methods becomes necessary with the aim of extending the preliminary results and correcting the wrong ones.

## III. CALORIMETRIC RESULTS

In a material having a hysteretic first-order transition, the magnetothermal history is crucial for the physical properties. Frequently, the determinations of variables by different procedures are put together and compared when they should not be, due to their particular history dependence. The calorimetric methods have been extensively discussed, sometimes without considering the actual variable that is really measured. The most common methods are as follows:

(1) Relaxation calorimetry, like in a physical property measurement system from Quantum Design. The true measured variable is the relaxation time $\tau = mC_{p,B}/k$ ($m$ is mass, $C_{p,B}$ is specific heat at constant field and pressure, and $k$ is thermal conductance to the surroundings) obtained from a fit of the temperature/time recording to an exponential decay of the sample temperature to the thermal bath. The thermal conductance $k$ is measured in another run with a standard sample of well-known heat capacity. In a first-order transition $\tau \to \infty$ and the data depart from an exponential curve.

(2) AC calorimetry. It measures the amplitude of the temperature oscillation when a periodic power is applied. This method cannot be applied in the temperature region with a phase change of first order.

(3) Differential scanning calorimetry (DSC). It consists of a relatively fast continuous heating or cooling of a small sample. The measured quantity is the heat power supplied, that is, the time derivative of the enthalpy ($H$). This method has a small precision because the sample is never in good thermal equilibrium, and is far away when a first-order transition occurs because, during the time range with phase coexistence, the real temperature is constant, but the temperature given by the measuring system varies continuously. It gives with precision the latent heat of the transition.

(4) Adiabatic calorimetry (ADC). The classical heat pulse method often uses massive samples and measures the temperature increment between two states of strict thermodynamic equilibrium when a given amount of heat is supplied to a sample, otherwise well insulated thermally. It is the most accurate and reliable, but a very slow and laborious method. It also has several drawbacks: In a first-order transition, when phase coexistence occurs, the relaxation time after a pulse is theoretically infinite, the actual waiting time for equilibrium is very long, and a good thermal insulation is difficult to maintain. The nominal heat capacity includes the real heat

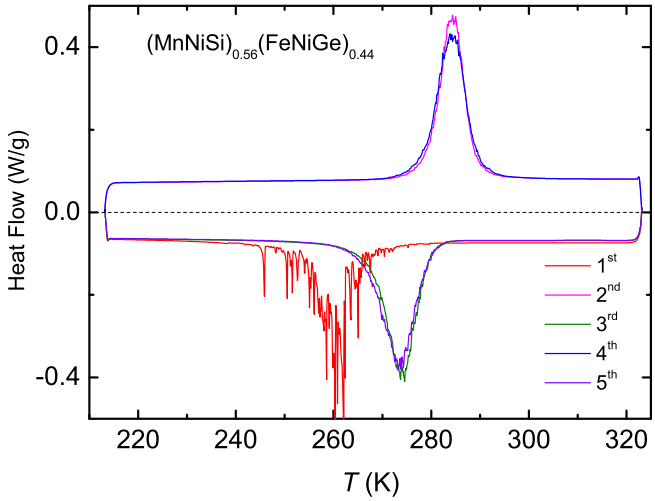


FIG. 1. Several DSC runs on $(MnNiSi)_{0.56}(FeNiGe)_{0.44}$, showing the difference between the first and the following coolings. The first, third, and fifth runs on cooling, and the second and fourth runs on heating.

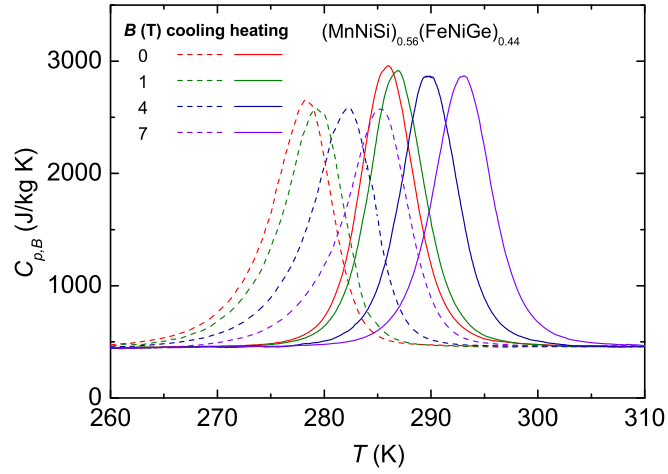


FIG. 2. Heat capacity on heating and cooling under several constant magnetic fields.

capacity of the present phases and the latent heat contribution when phase conversion occurs. Moreover, the ADC works only on heating.

(5) Thermograms [22]. This method, intermediate between DSC and ADC, is especially intended to study first-order transitions. It uses an adiabatic system where the sample is continuously and quasistatically heated or cooled, at typical rates around 2 mK/s, by conduction or radiation while the temperature/time evolution is recorded every few seconds. Calibrating the conduction and radiation powers, this method gives an enthalpy/time recording. The heat capacity is obtained numerically as $C_{p,B}(T,B) = (\partial H/\partial T)_{p,B}$. The method can be tested by checking the total enthalpy difference $\Delta H$ across the transition, determined by method 4, in a long pulse covering the full transition.

### A. Differential scanning calorimetry

Five DSC runs have been made at zero magnetic field, at rates of $\pm 10$ K/min, starting with a fresh sample in the hexagonal phase, preheated up to 323 K (Fig. 1). In the first cooling, the transition occurred at 262 K. It proceeded by avalanches, as indicated by the multiple peaks in the *heat flow/temperature* diagram. As usual in a polycrystalline bulk sample with anisotropic volume change, the internal stresses hinder the transition and the sample remains in an overcooled metastable phase. When a small part of the sample undergoes the transition, the interphase propagates rapidly to a relatively large volume. The avalanche stops because the released latent heat stabilizes the high temperature phase in the part of the sample that did not undergo the transition. As the temperature decreases, the system extracts heat from the sample until a new avalanche occurs, and so on until the entire sample is in the low temperature phase. On heating, the transition occurs at $T_{th} = 284.5 \pm 1$ K, where the maximum heat flow occurs for this heating rate. The same $T_{th}$ is observed in all heating runs. In all subsequent cooling runs the transition occurred at $T_{tc} = 274 \pm 1$ K.

The thermal shock at the transition breaks the sample into smaller powder grains. This relaxes the stresses and, in further cooling runs, every grain proceeds independently at a higher temperature and without avalanches. The latent heat, or enthalpy change at the transition is $L_h = 17.0$ J/g on heating and $L_c = 16.5$ J/g on cooling. Assuming the entropy jump $\Delta S \simeq L/T_t = 60$ J/kg K in both cases, similar to the value obtained from magnetization [14], via the CC equation, $\Delta S = -\Delta M(dB_t/dT_t) \simeq 55$ J/kg K. Actually, the classical CC equation is not strictly valid for this hysteretic transition and really $\Delta S > L/T_t$ due to the thermodynamic irreversibility of the transition, but the difference is less than 2% as we discuss below.

### B. Heat capacity

The heat capacity of $(MnNiSi)_{0.56}(FeNiGe)_{0.44}$ at zero magnetic field has been determined by ADC [method (4)] on a bulk sample of $m = 1.414$ g. We used heating and cooling thermograms [method (5)] at external fields $B = 0$, 1, 4, and 7 T to determine the enthalpy $H(T,B)$, taking $H = 0$ at 250.40 K as an arbitrary reference. The heat capacity $C_{p,B} = (\partial H/\partial T)_{p,B}$ is depicted in Fig. 2. Subtracting a proper base line, $C_{\text{base}}$, allows obtaining the latent heat, so-called "anomalous" contribution of the phase transition. Table I lists the main parameters deduced from the measurements. The transition temperatures on heating, $T_{th}$, or on cooling, $T_{tc}$, are

TABLE I. Transition temperatures $T_t$ (K), and jumps of enthalpy $L$ (J/g) and entropy $\Delta S$ (J/kg K) deduced from heat capacity data, on heating and cooling (subscripts $h$ and $c$), for several magnetic fields $B$ (T). $T_t$ is taken as the point of 50% phase conversion, or half anomalous enthalpy. Estimated errors are one unit of the last digit.

| $B$ | $T_{th}$ | $\Delta S_h$ | $L_h$ | $T_{tc}$ | $\Delta S_c$ | $L_c$ |
|---|---|---|---|---|---|---|
| 0.00 | 285.9 | 61 | 17.2 | 277.5 | 63 | 17.3 |
| 1.00 | 286.8 | 60 | 17.1 | 278.5 | 61 | 16.9 |
| 4.00 | 289.8 | 60 | 17.3 | 281.4 | 63 | 17.5 |
| 7.00 | 293.0 | 62 | 17.9 | 284.5 | 62 | 17.4 |

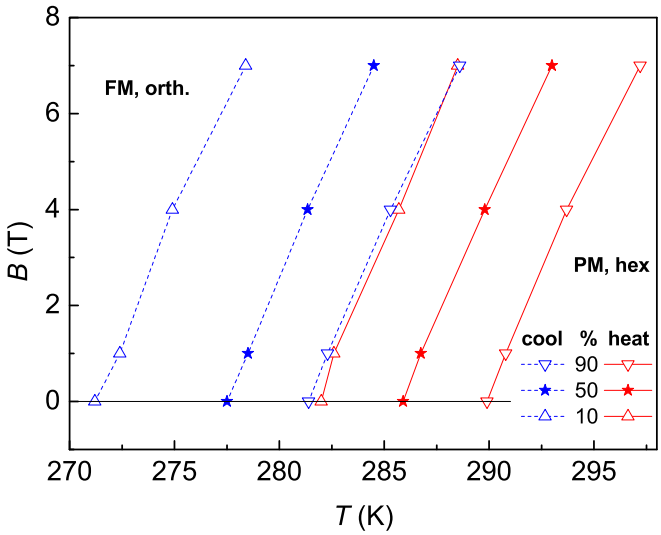


FIG. 3. $B/T$ phase diagram obtained from the thermograms [method (5)] at constant fields $B = 0$, 1, 4, and 7 T. Points of 10% ($\triangledown$), 50% ($\star$), and 90% ($\triangledown$) of the PM phase on heating (red symbols) and on cooling (blue symbols).

taken, for each field, as the point at which the percentage of each phase is 50%, which are deduced as the temperatures at which the anomalous enthalpy, $H_{\rm an}$, is one half of the total. There is a thermal hysteresis, $T_{th} - T_{tc} = 8.4$ K, practically independent of field. The transition temperature increases with the field with $dT_t/dB = 1.0$ K/T, on cooling and heating.

From the anomalous enthalpy, obtained at any temperature and field, the percentage $y$ of the PM phase can be deduced as

$$y(T,B) = \frac{100}{L(B)} \int_{T_0}^{T} [C_{p,B}(T,B) - C_{\rm base}(T)]dT, \qquad (3)$$

where $T_0$ is a low enough temperature to have pure FM state and $C_{\rm base}(T)$ is a linear nonanomalous baseline. The $B/T$ phase diagram (Fig. 3) is very similar to that of MnAs [19], although now, the existence of a critical point at high field and temperature cannot be inferred from the available data. The points of $y = 10\%$, 50%, and 90% of the PM phase in the transition process on heating and on cooling are indicated as symbols connected with lines.

This diagram, crucial to understand the results of MCE determinations, allows knowing the state of the sample and, particularly, the percentage $y$ of the PM phase for any field, temperature, and history. The curves of constant $y$ are very approximately parallel straight lines like those drawn in Fig. 3, where only three have been shown for clarity. Starting at low $T$ or high $B$, in pure FM state ($y = 0$) and moving to the right or downwards in the $B/T$ diagram, $y$, at any point $(T, B)$, is the corresponding value of the red constant $y$ line passing through this point. Starting in the PM state ($y = 100$) and moving to the left or upwards, the value of $y$ is given by the corresponding blue constant $y$ dashed line through the point.

Other thermal and magnetic histories can also be considered. For instance, starting in the FM state at $B = 0$ and moving to the right up to the 50% red curve. Then, moving upwards, the percentage of sample converted to PM state would start to transit back to FM state when crossing the 50% blue dashed line, for $B \simeq 8.3$ T. The rest of the sample never reached the PM state. We will show in Sec. IV that the experiments corroborate this behavior. This is the usual protocol followed for the determination of the isothermal magnetization. On increasing the field isothermally, there is no phase conversion if the maximum applied field is lower than 8.3 T. The MCE is then the normal value for a mixture of 50% FM and 50% PM phases, corresponding to the pure magnetic entropy change of each phase without any transition. A "giant" or "colossal" value of $\Delta S_T$ is, in this case, simply a wrong determination.

The entropy is conventionally deduced as

$$S(T,B) = S(T_0,B) + \int_{T_0}^{T} \frac{C_{p,B}(T)dT}{T}, \qquad (4)$$

where $T_0$ is a reference temperature at which the entropy value is known or has been arbitrarily assigned for $B = 0$. To determine $S(T_0, B)$ for different fields, direct measurements of $\Delta S_{T_0} = S(T_0, B) - S(T_0, 0)$ have been used, as explained below. Here we remark that, in a first-order transition with hysteresis, there is an irreversible entropy generated. $S(T, B)$ will be higher than the result of the right-hand side of Eq. (4). The entropy generated in a heating-cooling cycle covering the transition is $\Delta S_{\rm gen} \simeq 2E_{\rm diss}/T_t$, assuming equal dissipated energy on cooling and heating. $2E_{\rm diss}$ can be evaluated as the area of the hysteresis loop in an $S/T$ diagram. The result in our case is $E_{\rm diss} \simeq 0.015L$, which allows using the equal sign in Eq. (4) with only a small error. Also, $E_{\rm diss}$ is found to be almost constant with the field and the correction for irreversibility in the CC equation, Eq. (2), can be neglected.

The application of Eq. (4) for several magnetic fields allows knowing the entropy for every temperature and field. For every $B$ at any temperature within the transition region, the sample can be in different states of FM and PM fractions. The entropy, magnetization, and other extensive quantities should be computed considering not only the intensive variables $T$ and $B$ but also the percentages $y$ and $100 - y$ of each phase in thermal, mechanical, and magnetic equilibrium but not in the chemical one, since the chemical potential, or specific free energy, is not the same in both coexistent phases. The proportion $y$ depends on the path followed by the sample state in the $B/T$ diagram until reaching the given state. These considerations serve to analyze the apparently contradictory behavior of the sample in different experiments.

## IV. MAGNETOCALORIC EFFECT

The main variables summarizing the MCE, $\Delta S_T$ and $\Delta T_{\rm ad}$, can be obtained in three ways:

(1) $\Delta S_T \equiv S(T, B) - S(T, 0)$ from magnetization data, via the Maxwell relation, Eq. (1).

(2) $\Delta S_T$ from heat capacity data, through the entropy curves. Considering $\Delta T_{\rm ad} \simeq \Delta T_S$, it can be determined solving numerically for $\Delta T_S$ the integral equation

$$-\Delta S_T \equiv S(T,0) - S(T,B) = \int_{T}^{T+\Delta T_S} \frac{C_{p,B}(T,B)dT}{T} \qquad (5)$$

as shown graphically in Fig. 2 of [23].

(3) Directly measured. $\Delta S_T$ is measured as sketched in [24]. However, more details are given here, to clarify the

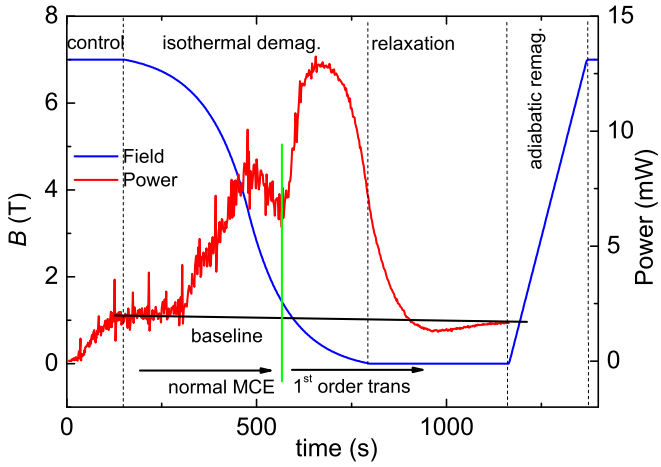


FIG. 4. Detail of a measurement of $\Delta S_T$ at $T = 290.83$ K, for decreasing $B$ from 7 T to 0.

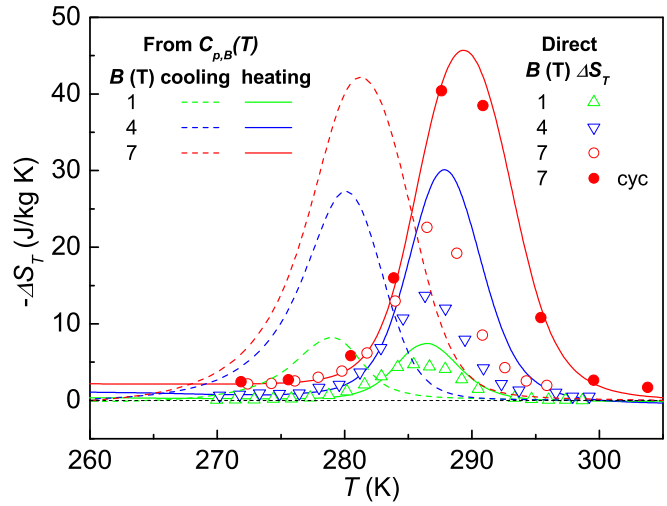


FIG. 5. $\Delta S_T$ obtained from heating and cooling thermograms, along with directly measured data on demagnetization. Solid lines: From heating thermograms. Dashed lines: From cooling thermograms. Open symbols: Direct determination via protocol 1. Solid symbols: Direct determination via protocol 2.

results. The sample is in a holder surrounded by an adiabatic screen in which the temperature is controlled to follow the sample temperature within 1 mK, ensuring thermal insulation. In these conditions, the magnetic field is decreased while heat is supplied to the sample by an electrical resistor with the controlled current to keep constant the sample temperature, closer than 0.05 K from a set point. The time integral of the power, $P(t)$, gives the supplied heat at constant temperature. The entropy change due to the magnetic field variation is then

$$\Delta S_T = \frac{1}{T}\int [P(t) - P_{\text{base}}]dt. \tag{6}$$

Figure 4 shows a typical recording of the magnetic field and the supplied power, $P(t)$, on an isothermal demagnetization in the phase transition region, made at $T = 290.83$ K, for a field variation from 7 T to 0. After heating the sample from the previous demagnetization made at 288.81 K up to the new set temperature under a field of 7 T, one can see several stages in the plot:

(a) Set point control (116 s $< t <$ 154 s). The control system keeps $B = 7$ T obtaining a base line, $P_{\text{base}} = 1.92$ mW, for the heating power. This base power is necessary to compensate for any deficit in thermal insulation. Actually, the temperature control is better if a small continuous heat leak is intentionally allowed. This heat loss is compensated by $P_{\text{base}}$.

(b) Isothermal demagnetization (154 s $< t <$ 798 s). The required heating power to maintain a constant temperature while $B$ decreases is supplied by the automatic controller. The field varies in a sigmoidal way to make easier the control by a proportional and integral procedure.

(c) Relaxation (798 s $< t <$ 1164 s). The system keeps $B = 0$ allowing the sample to reach equilibrium. Then, the system is ready for taking the field to 7 T and heating the sample to a new target temperature.

The supplied power during the isothermal demagnetization can be understood considering the phase diagram shown in Fig. 3. Initially, at $T = 290.83$ K and $B = 7$ T, the sample has a fraction in FM state which has the normal MCE for a ferromagnet [10], plus also some contribution from the majority PM phase. Therefore, $P(t) - P_{\text{base}}$ is approximately proportional to $-dB/dt$, having the maximum for $B = 3.5$ T, when this derivative is maximum. Below this field, $P(t)$ decreases until $B = 1.3$ T ($t = 565$ s) when the FM fraction starts to convert to PM state. This conversion involves a high latent heat and $P(t)$ needs to be high even for a small fraction of sample changing phase and a slow field variation. Finally, the magnetic field goes to 0 but the phase conversion continues until the equilibrium state is reached, since the high heat capacity and low diffusivity implies a long relaxation time in the phase conversion.

According to the phase diagram, the FM → PM phase conversion occurs only at low fields, when crossing the red line referred to in Fig. 3, corresponding to the state reached in the demagnetization prior to the last one. The fractions of sample having the transition line at higher fields did already convert in the previous demagnetizations up to 288.81 K. Considering the experiments at all temperatures, the overall picture is similar to that shown for $Ni_{50}CoMn_{36}Sn_{13}$ in Fig. 2(b) of [20] taking into account that, in this last case, the compound had inverse MCE and the slope of the constant $y$ lines was negative.

Figure 5 shows the results for $\Delta S_T$, obtained from heating and cooling thermograms, as the entropy difference $\Delta S_T = S(T, B) - S(T, 0)$. It also includes the direct measurements made using two protocols:

(1) Conventional, as shown in Fig. 4. That is, starting at a low temperature and maximum field, the sample is heated to an initial temperature; it is isothermally demagnetized while measuring the supplied power to maintain constant $T$; then, it is remagnetized and heated to the next desired temperature. With this protocol, the phase conversion in the transition region occurs on demagnetization at low field and could also occur on heating at constant field to the next set point, if the temperature interval was large enough.

(2) Thermally cycled. Everything is like in the previous protocol but, after demagnetization and before remagnetizing,

the temperature is decreased to a low value to ensure the transition of the entire sample to FM state. The sample is brought to the new desired temperature at the constant high $B$ and then isothermally demagnetized while measuring the power input.

One can observe in Fig. 5 that the results obtained following the conventional protocol, shown with open symbols, have quite smaller $|\Delta S_T|$ values than those deduced from the entropy curves on heating. This can be understood since, after every demagnetization, the fraction of sample which underwent the FM → PM transition did not go back to FM state on the new remagnetization due to the high hysteresis and the limited maximum field. On the contrary, making the measurement of $\Delta S_T$ following the protocol with thermal cycling, the sample state before demagnetization is the same as in the heating thermogram at 7 T and, just after demagnetization, its state is like the one obtained in the heating thermogram at 0 T. Consequently, the measured entropy difference is the same as the one deduced from thermograms, as shown in the experimental results for 7 T given in Fig. 5. We remark that the direct determination measures explicitly the heat really absorbed on demagnetization, which is the important quantity for magnetic refrigeration. This shows that a relatively simple heat capacity determination gives good values of $\Delta S_T$ without a laborious direct determination with thermal cycling.

## V. DISCUSSION

$(MnNiSi)_{0.56}(FeNiGe)_{0.44}$ has very similar properties to those of MnAs, with a magnetostructural transition of high latent heat, not having the toxic element As. A strong MCE has been reported with maximum $|\Delta S_T| \simeq 11.5$ J/kg K at 290 K for only 1 T, deduced from isothermal magnetization measurements, via the Maxwell relation [14]. Nevertheless, this result is an artifact due to an incorrect application of this relation. The direct determination of $|\Delta S_T|$ with the conventional protocol, measured as the real heat absorbed on demagnetization, gives much smaller results. The $|\Delta S_T|$ values obtained from heat capacity give higher results but also lower than those reported as derived via the Maxwell relation. Even so, $|\Delta S_T|$ reaches high values, making this compound very interesting with regard to applications in magnetic refrigeration.

As already mentioned, the conventional direct determinations without thermal cycling do not agree with those deduced from heat capacity via the entropy curves. This is due to the different sample history followed with the protocols used in each type of determination. When the direct $|\Delta S_T|$ data of a sample, cycled through the low temperature FM phase, are taken on demagnetization, the values agree with those deduced from $C_{p,B}$.

To discuss the values obtained from $M_T(B)$ data up to 1 T, measured at increasing temperatures [14], we plot them in Fig. 6, together with direct measurements using the conventional protocol, and also the results from heat capacity. $M_T(B)$ had been measured on another physical sample and, taking into account that the transition temperature depends very strongly on the composition, most probably a slightly different stoichiometry gave its transition 5.2 K above the values for our sample. Therefore, for comparison purposes,

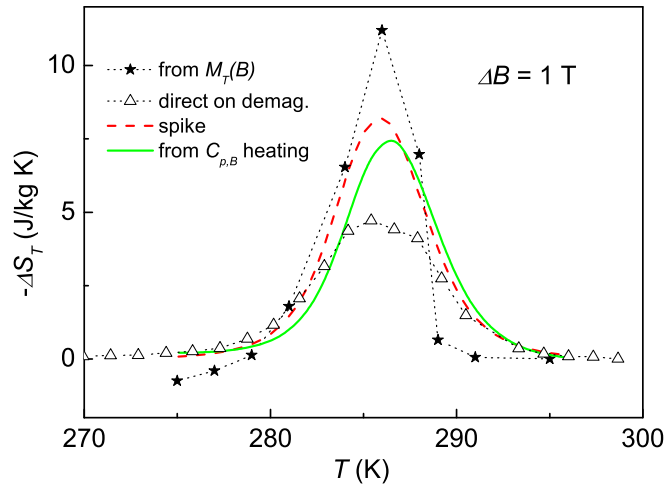


FIG. 6. $\Delta S_T$ for a field change of 1 T: From isothermal magnetization [14] (⋆). From direct determinations on demagnetization using the conventional protocol (Δ). From heat capacity on heating (green line). Calculated $\Delta S_{ex}$, named spike, with Eq. (7) (dashed red line).

the reported data from magnetization [14] have been shifted 5.2 K downwards.

Computing $\Delta S_T$ with a naive application of the Maxwell relation to isothermal $M_T(B)$ data, taken at increasing temperatures without cycling the sample to the PM state, leads to an extra term [19], so-called spike, given by

$$\Delta S_{\rm ex} = -\frac{C_{p,\rm an}(T, B=0)}{L}(M_F - M_P)B, \tag{7}$$

where $C_{p,\rm an}(T, B=0) = C_{p,B}(T, B=0) - C_{\rm base}(T)$ is the anomalous heat capacity at zero field, $L = \int C_{p,\rm an}(T, B=0)dT$ is the latent heat, $B$ is limited by the transition field $B_t$ from PM to FM, and $M_F - M_P$ is the magnetization difference between the FM and PM phases at temperature $T$, having a value $M_F - M_P \simeq 56.8$ A m$^2$/kg independent of $B$, taken from the plots of [14]. The direct measurements of $\Delta S_T$ with the nonthermally cycled conventional protocol give lower values.

Integrating Eq. (7) along the temperature of the transition anomaly, gives that the area under the spike is constant and proportional to the applied field, but limited to $B \leqslant B_t$.

$$\int \Delta S_{\rm ex} dT = -(M_F - M_P)B. \tag{8}$$

Therefore, in a small grain of sample, where the anomaly is narrower, the height of the $\Delta S_{\rm ex}$ spike should be greater than in a bigger sample. The values of $\Delta S_T$ in Fig. 6 obtained from magnetization data [14], had been measured in a much smaller sample than the one used for heat capacity and clearly the peak is narrower. These values, which really correspond to the spike from the $M_T(B)$ measurements, have therefore a higher peak than the spike computed with heat capacity data, as shown in Fig. 6.

According to the phase diagram, the fraction of sample converted from FM to PM state on heating to any temperature at zero field cannot return back to FM state by applying isothermally the weak field of 1 T. This backward transition would need a field higher than 8.3 T. The true isothermal

entropy decrement and the released heat upon isothermal magnetization up to 1 T correspond to the normal MCE of the mixture of FM and PM phases present in the initial mixed state, and it is small. The extra nonphysical term, $\Delta S_{ex}$, corresponds to the latent heat of the fraction of sample transformed at zero field during the heating to the new set point temperature, prior to the field increase. Therefore, the determination of $\Delta S_T$ made from isothermal magnetization measurements, using the commonly used protocol, does not correspond to the true isothermal entropy change.

It should be remarked that the Maxwell relation, correctly applied, is rigorously valid on the isothermal magnetization, since there is no phase conversion for a field increase up to $B = 1$ T. The problem is that the commonly used numerical calculation also includes the latent heat of the phase conversion during the heating prior to the magnetization. A procedure with the appropriate thermal cycling, as described above in protocol 2 for the case of demagnetizations, would have given correct results.

This calculation shows that the huge values obtained from isothermal magnetization are due, essentially, to the spike effect. Results reported for a compound with a close stoichiometry, $(MnNiSi)_{0.53}(FeNiGe)_{0.47}$ [15], gave the high value $-\Delta S_T = 70.1$ J/kg K for a field change of 5 T. It is due to the nonphysical spike artifact introduced by the naive application of the Maxwell relation to isothermal magnetization data using a nonthermally cycled protocol. The same remark can be made about the $\Delta S_T$ data reported for the Co alloys $(MnCoGe)_{1-x}(NiCoGe)_x$ [25] and $(MnNiSi)_{1-x}(FeCoGe)_x$ [26,27].

The results on our slightly different alloy, obtained from the entropy curves, found a maximum value $-\Delta S_{T,max} = 45.7$ J/kg K on demagnetization from 7 T, which is somewhat lower than the prediction given by the CC equation for the complete transition, $\Delta S = 55$ J/kg K, as it should be, because the phase diagram shows that there is not a complete phase conversion at any temperature for a field lower than 8.3 T.

## VI. CONCLUSIONS

The family of rare-earth free alloys $(MnNiSi)_{1-x}(FeNiGe)_x$ has a very strong magnetocaloric effect associated to the magnetostructural transition from the paramagnetic hexagonal phase to the ferromagnetic orthorhombic one, which can be induced by a moderate magnetic field. The MCE of the studied compound $(MnNiSi)_{0.56}(FeNiGe)_{0.44}$ is not as high as expected from values reported based on magnetization data through a naive application of the Maxwell relation but, even so, it is very strong.

The $B/T$ phase diagram has been deduced from calorimetric measurements. The thermal and magnetic history of different experimental protocols used in the literature has been analyzed, deducing their suitability to obtain reliable results for the magnetocaloric parameters.

A quantitative evaluation is given for the nonphysical $\Delta S_{ex}$, so-called spike, resulting from a very commonly used but incorrect application of the Maxwell relation to isothermal field dependent magnetization data.

Results of $\Delta S_T$ from calorimetric, magnetic, and direct measurements, using gradual temperature increments or complete cycles between the FM and PM phases, have been analyzed with reference to the phase diagram.

The isothermal entropy change, $-\Delta S_T$, has been explicitly measured as the heat absorbed on isothermal demagnetization. It results with values $-\Delta S_T > 40$ J/kg K between 287 and 291 K for $\Delta B$ from 0 to 7 T. From heat capacity data on heating, we obtained a maximum value $-\Delta S_{T,max} = 45.7$ J/kg K near 289 K for the same field change, $-\Delta S_{T,max} = 30$ J/kg K for $\Delta B = 4$ T, and $-\Delta S_{T,max} = 7.4$ J/kg K for $\Delta B = 1$ T, which compares very favorably with other families for similar field variations: MnAs with $-\Delta S_{T,max} = 28.2$ J/kg K, for $\Delta B = 6$ T [5], $Gd_5Si_2Ge_2$ with $-\Delta S_{T,max} = 14.0$ J/kg K for $\Delta B = 5$ T [24], obtained with the same rigorous method, and $La(Fe,Si)_{13}H$ with $-\Delta S_{T,max} \simeq 25$ J/kg K for $\Delta B = 5$ T [4].

The only drawback is the high hysteresis of 8.4 K. However, it could be reduced in many compounds by a small doping with other elements, as in the closely related case of MnAs, which has a hysteresis of 10 K, but replacing 10% of As with Sb it decreases to 1 K with only a small reduction of $|\Delta S_T|$ [28]. Recently, it has been found in $(MnNiSi)_{0.67}(Fe_2Ge)_{0.33}$ that application of pressure reduces considerably the hysteresis, maintaining high $\Delta S_T$ values [29].

The observed $\Delta S_{T,max}$ of our compound is lower than expected from the Clausius-Clapeyron equation. Taking into account that the CC equation gives the entropy jump at the transition when the phase coexistence line is crossed, without including further changes produced before or after crossing this line, we conclude that the transition is not complete even for a field variation of 7 T, due to having a high field hysteresis of 8.3 T. Therefore, a derived compound without hysteresis could even increase the entropy change with respect to the present alloy. Consequently, this family is very interesting and promising for its possible application in magnetic refrigeration.

## ACKNOWLEDGMENTS

The authors acknowledge funding from the Ministerio de Ciencia, Innovación y Universidades (MICINN) and FEDER, Project No. MAT2017-86019-R.

[1] W. F. Giauque and D. P. MacDougall, Phys. Rev. **43**, 768 (1933).

[2] S. Yu. Dan'kov, A. M. Tishin, V. K. Pecharsky, and K. A. Gschneidner, Jr., Phys. Rev. B **57**, 3478 (1998).

[3] V. K. Pecharsky and K. A. Gschneidner, Jr., Phys. Rev. Lett. **78**, 4494 (1997).

[4] A. Fujita, S. Fujieda, Y. Hasegawa, and K. Fukamichi, Phys. Rev. B. **67**, 104416 (2003).

[5] L. Tocado, E. Palacios, and R. Burriel, J. Therm. Anal. Calorim. **84**, 213 (2006).
[6] O. Tegus, B. Fuquan, W. Dagula, L. Zhang, E. Brück, P. Z. Sia, F. R. de Boer, and K. H. J. Buschow, J. Alloys Compd. **396**, 6 (2005).
[7] T. Tohei, H. Wada, and T. Kanomata, J. Magn. Magn. Mater. **272-276**, E585 (2004).
[8] R. Burriel, L. Tocado, E. Palacios, T. Tohei, and H. Wada, J. Magn. Magn. Mater. **290-291**, 715 (2005).
[9] T. Krenke, E. Duman, M. Acet, E. F. Wassermann, X. Moya, Ll. Mañosa, and A. Planes, Nat. Mater. **4**, 450 (2005).
[10] A. M. Tishin and Y. I. Spichkin, *The Magnetocaloric Effect and its Applications* (IOP Publishing Ltd., Bristol, UK, Philadelphia, 2003).
[11] V. Franco, J. S. Blázquez, J. J. Ipus, J. Y. Law, L. M. Moreno-Ramírez, and A. Conde, Prog. Mater. Sci. **93**, 112 (2018).
[12] N. T. Trung, V. Biharie, L. Zhang, L. Caron, K. H. J. Buschow, and E. Brück, Appl. Phys. Lett. **96**, 162507 (2010).
[13] N. T. Trung, L. Zhang, L. Caron, K. H. J. Buschow, and E. Brück, Appl. Phys. Lett. **96**, 172504 (2010).
[14] C. L. Zhang, D. H. Wang, Z. D. Han, B. Qian, H. F. Shi, C. Zhu, J. Chen, and T. Z. Wang, Appl. Phys. Lett. **103**, 132411 (2013).
[15] P. Dutta, S. Pramanick, S. Chattopadhyay, D. Das, and S. Chatterjee, J. Alloys Compd. **735**, 2087 (2018).
[16] L. M. Moreno-Ramírez, A. Díaz-García, J. Y. Law, A. K. Giri, and V. Franco, Intermetallics **131**, 107083 (2021).
[17] K. Deepak and R. V. Ramanujan, J. Alloys Compd. **743**, 494 (2018).
[18] W. Hanggai, O. Tegus, H. Yibole, and F. Guillou, J. Magn. Magn. Mater. **494**, 165785 (2020).
[19] L. Tocado, E. Palacios, and R. Burriel, J. Appl. Phys. **105**, 093918 (2009).
[20] E. Palacios, J. Bartolomé, G. F. Wang, R. Burriel, K. Skokov, S. Taskaev, and V. Khovaylo, Entropy **17**, 1236 (2015).
[21] A. Planes, Ll. Mañosa, and M. Acet, J. Phys.: Condens. Matter **21**, 233201 (2009).
[22] E. Palacios, J. J. Melero, R. Burriel, and P. Ferloni, Phys. Rev. B **54**, 9099 (1996).
[23] E. Palacios, M. Evangelisti, R. Sáez-Puche, A. J. Dos Santos-García, F. Fernández-Martínez, C. Cascales, M. Castro, R. Burriel, O. Fabelo, and J. A. Rodríguez-Velamazán, Phys. Rev. B **97**, 214401 (2018).
[24] E. Palacios, G. F. Wang, R. Burriel, V. Provenzano, and R. D. Shull, J. Phys: Conf. Seri. **200**, 092011 (2010).
[25] C. L. Zhang, H. F. Shi, E. J. Ye, Y. G. Nie, Z. D. Han, and D. H. Wang, J. Alloys Compd. **639**, 36 (2015).
[26] T. Samanta, D. L. Lepkowski, A. U. Saleheen, A. Shankar, J. Prestigiacomo, I. Dubenko, A. Quetz, I. W. H. Oswald, G. T. McCandless, J. Y. Chan, P. W. Adams, D. P. Young, N. Ali, and S. Stadler, J. Appl. Phys. **117**, 123911 (2015).
[27] T. Samanta, P. Lloveras, A. U. Saleheen, D. L. Lepkowski, E. Kramer, I. Dubenko, P. W. Adams, D. P. Young, M. Barrio, J. Ll. Tamarit, N. Ali, and S. Stadler, Appl. Phys. Lett. **112**, 021907 (2018).
[28] H. Wada, T. Morikawa, K. Taniguchi, T. Shibata, Y. Yamada, and Y. Akishige, Physica B **328**, 114 (2003).
[29] D. Clifford, V. Sharma, K. Deepak, R. V. Ramanujan, and R. Barua, IEEE Trans. Magn. **57**, 2500405 (2021).

*Correction:* The fourth sentence of the abstract and the second sentence of the first paragraph of Sec. II contained errors in wording and have been fixed. The last two column headings in Table I contained errors and have been fixed. New Reference [13] was added and subsequent references have been renumbered.